

# A HYBRID APPROACH TOWARDS SEGMENTATION OF RANGE IMAGES

Alan Wui Tze Lim, Eam Khwang Teoh and Dinesh P Mital  
 School of Electrical and Electronic Engineering  
 Nanyang Technological University  
 Nanyang Avenue  
 Singapore 2263  
 Republic of Singapore

## Abstract

This paper presents a technique for the segmentation of range images. It tends to be a hybrid approach that combines edge detection and region growing techniques toward accomplishing the task of segmentation. The surface coherency property of range data provided an important attribute, which enabled the improvisation of extrinsic knowledge regarding the types of surface primitives existing within an image. The cross-breeding approach produces a segmentation map and an edge map. Edges detected by such a method possessed good localisation property. The incorporation of region growing process eliminates internal micro edges and produces a segmentation map. These two maps would undoubtedly be of great value to the higher level recognition process.

## 1 Introduction

The advancement in the technology of range scanning devices, have enabled a breakthrough in accurate, reliable and stable acquisition of range data [1, 2].

Range image tends to provide 3-D perspective view of an object as well as conveying information on the various compound surfaces that made up the object. For the past few years, there have been an increased use of range images for inspection, object recognition and in autonomous guided vehicles (AGV) [3, 4]. The stability of range data has also brought about the trend in applying Computer Aided Design (CAD) technique for the modelling of objects based upon the acquired range data [5].

The modern approach has been adopted towards accomplishing the segmentation task; that is, it tends to be a hybrid approach of combining both the traditional edge detection and region homogeneity based techniques for accomplishing the region partitioning task. Unlike intensity images, range data geometri-

cally captures the surfaces or shapes of objects within a scene, i.e there is a coherency between the surfaces of an object and the data format of range images. As a result of its incorporation within the hybrid method, problems encountered by either technique may be minimised and improved. The cross-breeding approach produces a segmentation map and an edge map. In addition, the edge map conveys  $C^0$ , continuity information while the segmentation map may provide information on adjoining surfaces that resulted in the

formation of edges as well as defining boundary conditions.

The subject addressed by this paper is primarily on segmentation. It should be emphasized that the process aimed for a segmentation map that does not only provide accurate partitioning of regions, but also provide descriptive information on the various types of surface regions detected. In addition, in the approach taken, we have also emphasised on accurate localisation of edges since CAD modelling assumed surface joint to be  $C^1$  continuous; and as such edges is vital towards catering boundary conditions to the surface modelling process.

## 2 Philosophy of the Algorithm

Figure 1 shows a simplified flow chart of our algorithm. The following sections present a hybrid method that combine region growing and one dimensional edge detection processes. The region growing process served the purpose of fusing neighbouring pixels of similar construct into regions. The contour of each region provides evidence of instability, which may be as a result of noise or caused by the presents of an edge. Based upon the estimated direction as provided by the outline of each region, a third order orthogonal polynomial curve was fitted; the least square error curve would then be used to hypothesize or for the detection of edge points.

The attributes utilised by the region growing process were obtained by convolving the raw image with differential operators of different sizes.

### 2.1 Extracting Seedlings

The very first task involved in our algorithm was the extraction of seedlings. Each seed region should be isolated and should be far enough inside the boundaries of primitive surfaces. The fundamental purpose of such an action was to extract groups of regions which were stable, in the sense that the fit error and surface normal angular deviation were small. The seed regions would then be grown into bigger regions until the invaded pixels show signs of instability.

Seedlings were acquired from eroding a coarse segmentation map,  $sgn(x, y)$ , obtained by convolving (denoted by  $*$ ) each image pixel  $f(x, y)$ , with the Laplacian of Gaussian  $\nabla^2 G(x, y)$  operator;

$$s(x, y) = f * g, \quad (1)$$

$$\text{sgn}(x, y) = \begin{cases} +1 & \text{if } s(x, y) > \epsilon, \\ 0 & \text{if } s(x, y) = \epsilon, \\ -1 & \text{if } s(x, y) < \epsilon. \end{cases} \quad (2)$$

where  $\epsilon$  has been set to 0, and  $\sigma$  of the utilised LoG operator has been set to 2.8, i.e this resulted in a formation of a  $17 \times 17$  mask. It is to our believe that our approach in using the LoG operator as a segmentation tool is rather unique. It was found that regions are formed even though the edge boundaries are very weak.

Regions depicted by the sign distribution map,  $\text{sgn}(i, j)$ , were subsequently eroded eight times. This was to eliminate regions which were small and unstable. The remaining regions were further eroded or dilated to a region size of 40 or 20 pixels respectively. The pixels within each remaining region may be considered to be homogeneous in property not only to the particular primitive region it belonged to, but also to the primitive surface that it resided in.

## 2.2 Region Growing Process

As outlined above, each of the extracted seedlings were then grown into bigger region based upon three attribute maps, i.e  $\mathcal{E}(x, y)$ ,  $\aleph(x, y)$  and an KH-map.

Note, the first two attribute maps have the prime responsibility of conveying information on the smoothness of a patch rather than for detecting edges. The third attribute map has the prime responsibility of conveying surface shape information.

The attribute maps were obtained by convolving the raw image with convolution masks which were derived

using least square technique [6]. The size of the mask was  $5 \times 5$  and the basis equation assumed a biquadratic equation of the form,

$$\hat{f}(x, y) = ax^2 + by^2 + cxy + dx + ey + f, \quad (3)$$

where the squared fit error is given by,

$$\epsilon_f(x, y) = |\hat{f}(x, y) - f(x, y)|^2. \quad (4)$$

The angular difference  $\theta$ , between two adjacent surface normals,  $n_1$  and  $n_2$ , may be computed as follows [7],

$$\theta = \arccos(n_1 \cdot n_2). \quad (5)$$

The normal map  $\aleph(x, y)$  was then binarised by noting the maximum angular difference  $\theta_{max}$  between adjacent surface normals within a  $3 \times 3$  mask. That is,

$$\aleph(x, y) = \begin{cases} 1 & \theta_{max}(x, y) \geq \theta_t, \\ 0 & \theta_{max}(x, y) < \theta_t, \end{cases} \quad (6)$$

where  $\theta_t$  has been set to  $\frac{\pi}{95}$ .

The squared fit error map was also binarised but the threshold  $\epsilon_t$ , was empirically determined by the following criteria:

- If the maximum square fit error  $\epsilon_{max}$ , within the seed region falls within the range of 0.189 <

$\epsilon_{max} < 1.89$ , then the threshold  $\epsilon_t$  is set to  $\epsilon_{max}$ ; else,  $\epsilon_t$  would be set to the extreme value, i.e either 0.189 or 1.89.

Similarly, based upon the estimated  $\epsilon_t$ , a binarised edge map  $\mathcal{E}(x, y)$  was obtained.

$$\mathcal{E}(x, y) = \begin{cases} 1 & \epsilon_f(x, y) \geq \epsilon_t, \\ 0 & \epsilon_f(x, y) < \epsilon_t. \end{cases} \quad (7)$$

The intrinsic surface property map, KH-map, was formulated by noting the sign of K and H. From the theory of differential geometry, it is noted that surfaces may be uniquely classed as according to the sign of gaussian K and mean H curvatures [8, 9, 10].

Basically, this is a scheme adopted from P.J. Besl [3, 9]. Eight types of surfaces, as shown in table 1, may be classified as according to the sign of mean H and gaussian K curvatures. K and H may mathematically be determined by the following equations:

$$K = \frac{f_{uu}f_{vv} - f_{uv}^2}{(1 + f_u^2 + f_v^2)^2} \quad (8)$$

$$H = \frac{1}{2} \frac{(1 + f_v^2)f_{uu} + (1 + f_u^2)f_{vv} - 2f_u f_v f_{uv}}{(1 + f_u^2 + f_v^2)^{2/3}} \quad (9)$$

Table 1: Surface classification based upon the sign of H and K.

	$K > 0$	$K = 0$	$K < 0$
$H < 0$	Peak	Ridge	Saddle Ridge
$H = 0$	(none)	flat	Minimal
$H > 0$	Pit	Valley	Saddle Valley

Based upon the  $\mathcal{E}(x, y)$  and  $\aleph(x, y)$  attribute maps, each seedling would be grown until a stage is reached where the number of invaded neighbouring pixels proved to be small; where stability of region here refers to smoothness, i.e the particular pixel has a value of 0 in both the attribute maps.

Due to the erosion process employed, it was noted that a single primitive surface region may contain several seedlings scattered across its surface. Consequently, the growing routine resulted in multiple label within a surface region. Hence, the primary function of the KH-map was responsible for judging whether neighbouring labelled regions should be allowed to fuse. The intrinsic surface type of each region were computed through a histogramming technique of selecting the surface-type tag with the highest count.

Once each seedlings has been grown, the resultant region maps were then copied and complemented; further seedlings and new regions were acquired by repeating the seed extraction and region growing algorithms with one minor modification, that is, the complemented region map was eroded 4 times instead of 8 times. The newly acquired regions were then registered in the former region map. The repetition of the processes was to acquire those seedlings that might have been lost due to over-erosion. By now, all (so called) stable re-

gions have been registered. The newly formed region map was then labelled and passed to the edge detection process.

### 2.3 Edge Detection

Traditionally, edge detection has proved important to image analysis. Likewise, it is important here; that is for providing the necessary guidance to the region growing process.

In our approach, we have regarded the edge detection process as a curve fitting problem. We have assumed that the surfaces involved are *piecewise-smooth graph surfaces*. Therefore, along the domain of a 1-D surface, the rate of change of error fit should remain constant. In other words, a sudden increment or decrement in the rate of change in fit error signifies that an edge is present.

The basis equation used for the 1-D curve fitting process was an orthogonal polynomial function, that satisfy the three term recurrence relationship [11],

$$p(x) = a_0\varphi_0 + a_1\varphi_1 + a_2\varphi_2 + a_3\varphi_3, \quad (10)$$

where,

$$\varphi_i(x) = (x - b_i)\varphi_{i-1}(x) - c_i\varphi_{i-2}(x), \quad (11)$$

and the constant coefficients  $b_i$  and  $c_i$ , are defined by the inner product of the basis functions over the domain of the functions.

$$b_i = \frac{\langle x\varphi_{i-1}, \varphi_{i-1} \rangle}{\langle \varphi_{i-1}, \varphi_{i-1} \rangle}, \quad (i = 1, 2, \dots) \quad (12)$$

$$c_i = \frac{\langle x\varphi_{i-1}, \varphi_{i-2} \rangle}{\langle \varphi_{i-2}, \varphi_{i-2} \rangle}, \quad (i = 2, 3, \dots) \quad (13)$$

with  $c_1 = 0$ ,  $\varphi_{-1} = 0$  and  $\varphi_0 = 1$ .

The fit error was defined by the equation,

$$\epsilon_{fit} = p(x) - f(x). \quad (14)$$

The curve fitting process was carried out at each pixel along the contour of the grown region, in the direction that is perpendicular to the estimated edge direction. Edge points were detected as according to the following rule:

- If a zero crossing (ZC) or a peak of significant height is encountered in the  $\frac{\delta\epsilon_{fit}}{\delta x}$  curve, then the position of the edge is taken to be at the point where ZC occurs or otherwise, the point where the extrema resides.

Each edge point encountered was registered in an Edge map,  $\mathcal{I}(x,y)$ . The  $\mathcal{I}(x,y)$  map was then passed to a routine that tends to employ multiple 3x3 or 5x5 edge mask for removing isolated and thus nonlogical (false) edge points, so as to refine any edge connectivity defects.

Once the edge refinement process is completed, the  $\mathcal{I}(x,y)$  map would be utilised to limit the growth of regions that were formerly discovered. Finally, an un-

conditional growth was allowed such that a labeled segmentation map was formed.

## 3 Implementation and Results

As noted, the algorithm outlined above tends to produce two maps, that is an edge map and a segmentation map. We have tested the algorithm based on range images that were supplied by Michigan State University. The algorithm on the whole performed well. Due to the limitation in space, only one set of results is presented. More results can be found in [14].

The results on a commonly encountered objects are displayed in line plot form in figure 2. The object in figure 2 is a "wye-joint" of a plumbing part. The figure on the left hand side displayed the edge map while that on the right displayed the segmentation map. Note that, the segmentation map tends to be very well formed even though the boundaries that lie on the central piece were not fully detected.

## 4 Discussion

Edges detected by the curve fitting algorithm tend to possess good localisation property. The number of points used in the curve fitting process plays an important role, i.e. basically as more points are employed, immunity of the process to the effect of noise increases. This is also reflected by the size of the convolution masks (5x5) that were employed for building the  $\mathcal{R}(x,y)$  and  $\mathcal{E}(x,y)$  maps. Note that apart from the KH-map, the attribute maps utilised have not undergone any filtering process. The pre-smoothing filter employed for formulating the KH-map was that of a 7x7 binomial filter.

Conventional method for edge detection was not utilised because with the employment of a one-dimensional mask, edge sensitivity and edge localisation may be significantly improved. This is one major characteristic of the Canny operator, see [12]. It also avoids the smoothing of edges or to be more precise, the smoothing of surface joint.

The region growing process served two purposes, i.e. to eliminate internally broken micro edges and to artificially ensures outline connectivity. In fact, the finding of Huble and Wiesel [13] and the evidence that the stereoscopic nature of the human visual system actually induces a region growing process that analyse surface curvatures, inspired us to adopt a hybrid approach towards edge detection and image segmentation. It should be noted that it would be impossible to achieve accurate border reconstruction if the overall process have not had any slightest hint on where the boundaries resided. Moreover, the good localisation property of the edge detection scheme further enhances accuracy of the constructed boundaries.

Finally, it should be noted that in order to obtain accurate partitioning of surfaces, intrinsic surface property is imminent. The inclusion of such property does not only prevent false fusage, but also convey information on the *surface-type* of each region. In other words,

surface coherency or geometrical concept of surfaces implies the inclusion of surface properties, be it intrinsic or extrinsic.

## 5 Conclusion

In this paper, we have presented a hybrid approach towards edge detection and image segmentation. Undoubtedly, the resultant maps would prove valuable to the higher level recognition process. Our experimental results show that edge detected and regions partitioned tend to have good localisation property.

One could extend the work done here into generating a segmentation map with descriptive value by considering integrating other sensory information or geometrical attributes, so as to make the overall segmentation process more robust and reliable.

## References

- [1] C. M. Bastuscheck, "Techniques for real-time generation of range images," in *Proc. IEEE CVPR*, pp. 262-268, 1989.
- [2] M. Rioux, F. Blais, J. A. Beraldin, and P. Boulanger, "Range imaging sensors development at nrc laboratories," in *IEEE Proc. Workshop on Interpretation of 3D Scenes*, pp. 154-160, November 1989.
- [3] P. J. Besl and R. Jain, "Range image understanding," in *IEEE Proc. CVPR*, pp. 226-233, 1985.
- [4] J. P. Brady, N. Nandhakumar, and J. K. Aggarwal, "Recent progress in the recognition of objects from range data," in *Proc. IEEE 9th Int. Conf. on Pattern Recognition*, pp. 85-92, 1988.
- [5] P. J. Flynn, *CAD-Based Computer Vision: Modelling and Recognition Strategies*. PhD thesis, Michigan State University, 1990.
- [6] R. M. Haralick and L. Watson, "A facet model for image data," *Computer Graphics and Image Processing*, vol. 15, pp. 113-129, 1981.
- [7] P. J. Besl and R. C. Jain, "Segmentation through variable-order surface fitting," *IEEE Trans Pattern Anal. Machine Intell.*, vol. 10, pp. 167-192, March 1988.
- [8] I. D. Faux and M. J. Pratt, *Computer Geometry for Design and Manufacturing*. New York: Ellis Horwood, 1979.
- [9] P. J. Besl, *Surfaces in Range Image Understanding*. New York: Springer-Verlag, 1986.
- [10] J. M. Beck, T. Farouki, and J. K. Hinds, "Surface analysis methods," *J. IEEE CGA*, pp. 18-36, 1986.
- [11] S. Yakowitz and F. Szidarovszky, *An Introduction to Numerical Computations*, pp. 297-322. Macmillan Publishing Company, New York, 1989.
- [12] J. Canny, "A computational approach to edge detection," *IEEE Trans Pattern Anal. Machine Intell.*, vol. 8, pp. 679-798, November 1986.
- [13] D. H. Huble and T. N. Wiesel, "Receptive fields, binocular interaction and functional architecture in the cat's visual cortex," *Journal of Physiol. Lond.* 160, pp. 106-154, 1962.
- [14] W. T. Lim, "A Hybrid Approach Towards the Segmentation of Range Images for 3-D Object Recognition," M. Eng Thesis, Nanyang Technological University, Singapore, 1992.

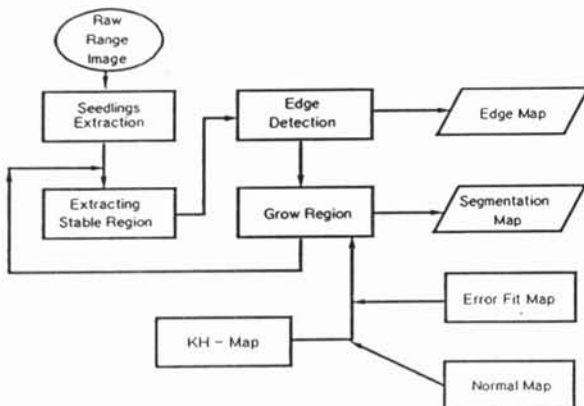


Figure 1: A simplified flow chart depicting the hybrid algorithm.

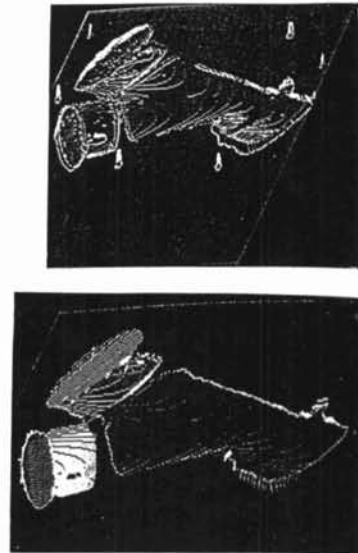


Figure 2: Edge and segmentation maps for the wye-joint.